

# PHOENICS News

Winter 2014/15



PHOENICS – YOUR GATEWAY TO CFD SUCCESS

## PHOENICS User Day at CHAM Japan



### Delegates

#### Presentations included:

- 1) *Proposed improvement to the thermal environment of a steel forging plant by CFD Simulation*, Mr Takeshi Takenaka, e-tech.
- 2) *Plant Design using PHOENICS*, Ms Mau Watanabe, Nisso Engineering Company Limited.
- 3) *A Simulation Study on Leaking Hydrogen Dispersion in a partially Open Space using Parallel PHOENICS* Mr Hisayoshi Tsukikawa, Kyushu University.
- 4) *PHOENICS Simulation to achieve High Efficiency and Low Combustion Emissions in a Bark Boiler*, Professor Kazushiga Kikuda & Mr Yuki Tatekura, Tomokomai National College of Technology
- 5) *Implementing the THINC Scheme in to the Free Surface Model of PHOENICS*, Mr Bin Xia, Tokyo Institute of Technology
- 6) *The effect of Turbulence on the Air Curtain of a Cold Show Case*, Professor Yoichi Shiomi, Ryukoku University.

CHAM Japan held a User Day in October at the Tokyo International Forum. It was attended by some 50 PHOENICS Users.

For further information contact CHAM Japan:

web: [www.phoenics.co.jp](http://www.phoenics.co.jp)

Email: [customer@phoenics.co.jp](mailto:customer@phoenics.co.jp) or

CHAM: [sales@cham.co.uk](mailto:sales@cham.co.uk).

## Model-Based Observational Analysis of a Flight-Quality LOX/Multi-fuel Rocket Engine with the PHOENICS CFD Code

P. M. Sheaffer and R. Ornellas  
The Aerospace Corporation  
2310 E. El Segundo Blvd. - M2/266  
El Segundo, CA 90245

November 14, 2014

### Abstract

*It can be said that we have entered the Model/Simulation Age; for example, CAD/CAE, FDTD (Finite-Difference-Time Domain), and multi-physics simulations have attained unprecedented accuracies on complex systems. Knowledge of the Earth's climate system is growing at an unprecedented rate and solid carbon (ie soot) has emerged as a significant anthropogenic forcing agent [1,2].*

*Advertised increases in "entertainment-related" international suborbital flights have the potential for injecting black carbon into the lower stratosphere where it is persistent. However, a quantitative understanding of soot generation in launch vehicles has not been a focus of research in recent decades.*

*We use the PHOENICS [3] code to explore the flows and chemistry of one type of operational rocket combustion chamber. Recent theoretical and laboratory studies exist [4,5], but we believe we are relatively unique in comparing our data to observations of a flight-grade LOX/ hydrocarbon engine in the 4,000 lbf thrust size class [6], and the improvements in CFD codes and computers suggests further study will be fruitful for understanding this potential contribution to anthropogenic climate-forcing.*

### Introduction

Although mathematically predicted since the time of Svante Arrhenius and Thomas Chamberlin, modern models make it increasingly clear that significantly perturbed climate dynamics may result in serious impacts

on globalized civilization within this century. Modern assessments conclude that black carbon is a primary concern [1,2,7] due to its long persistence above the troposphere and on snow, as well as its spectral character (ie solar visible/UV absorption). Black carbon *within* the troposphere is a short-lived climate forcing agent (eg "brown clouds") since it is removed rapidly by precipitation [8], thus being much more amenable to source-mitigation than molecular species such as CO<sub>2</sub> and CH<sub>4</sub>.

On the other hand, surprisingly little is known about the fate of the mass released by operational space-launcher combustion chambers, in particular with respect to *film cooling fractions* [4,9,10]. Mass flows of film coolants range from approximately 3 percent to over 10 percent of total first-stage launch vehicle fuel mass.

We note that there are 'evident soot flows' (eg Figure 1) which result from such engines, but there is almost no clear information on the *actual* soot fractions, and it appears immediately unreasonable to expect that all film coolant fuel is converted to low molecular weight species (eg CO, water) and soot without impacting the latent-heat dominated wall-cooling efficacy of these flows.

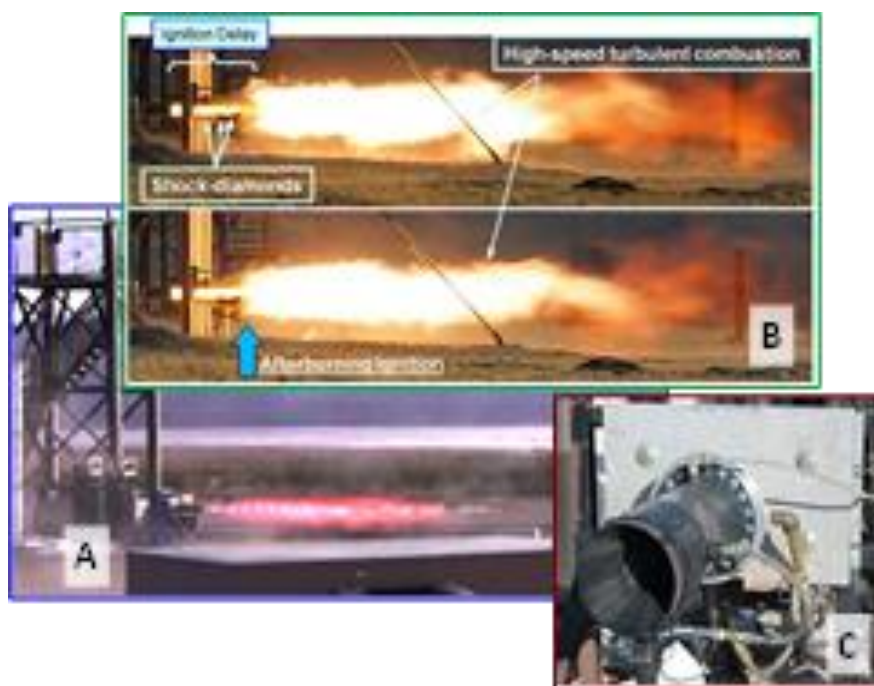
### Experimental

An illustration of the EPG Space 4,000 lbf thrust engine [6] is shown in Figure 1, operating with either LOX/kerosene or LOX/methanol, as noted.

Methanol has unusually low soot forming potential due to the absence of C-C bonds and the presence of bonded oxygen. It also has an unusually large latent heat of vaporization (4 x that of kerosene), supporting up to a 7.5% decrease in first-stage total fuel mass required to achieve similar combustion chamber and throat film-cooling.

A PHOENICS model, as shown in Figure 2, (page 3) can be run both with a complex thermo-chemical data base to assess chemical reaction rates and species distributions; and as a multi-phase non-reacting flow, to assess the flow topology with the increased fidelity of turbulence modelling, improved shock-capturing, and the use of the PHOENICS cut-cell solver PARSOL for capturing the nozzle geometry on the structured background mesh.

**Figure 1.** Several views of the 7-inch diameter, 4,000 lbf thrust LOX/multifuel research engine [4]. A – Engine in operation with LOX/methanol; B – Engine in operation with LOX/kerosene; C – View of engine immediately after firing. The complexity of the post-nozzle flow is evident in the notes on the images.





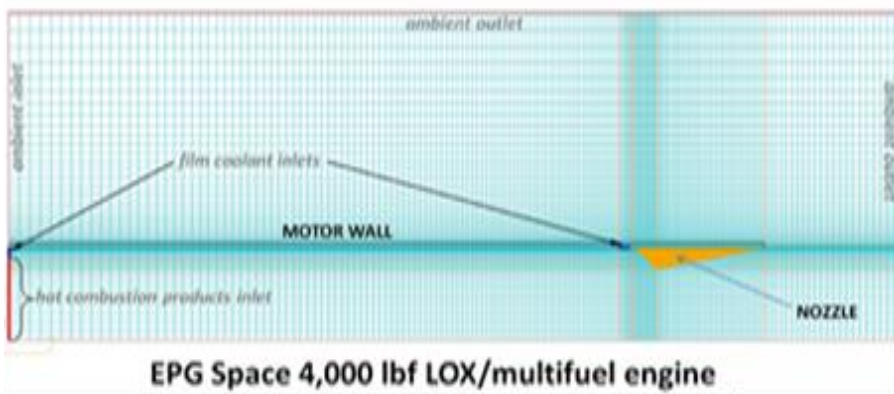


Figure 2. Solution domain for EPG engine combustion chamber. There are two film coolant inlets, the LOX/fuel injector film coolant on the left, and the nozzle coolant on the right

Figure 3 shows a solution obtained with fully compressible multiphase flows and turbulence, with and without chemistry activated. The persistence of the wall coolant down the length of the combustion chamber is evident. We also note, in consonance with recent literature [4,5], that the film coolant boundary layer is sensitive to both the turbulence model used and the magnitude of turbulence in the internal engine flows.

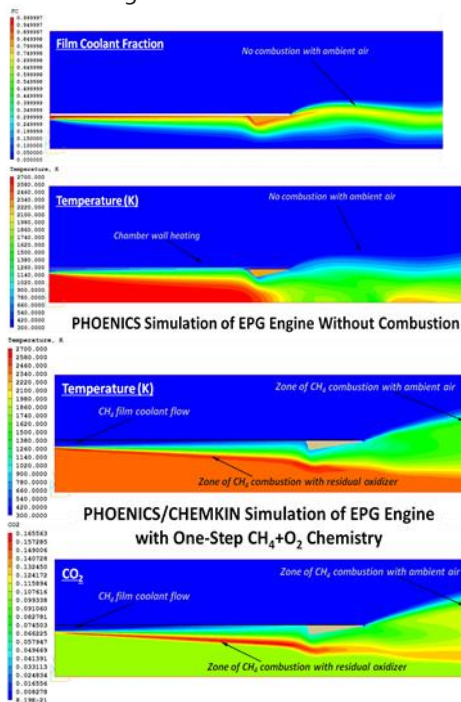


Figure 3. Converged solutions for the entire engine/exhaust system without chemistry included. The  $k-\epsilon$  turbulence model is used. Converged solutions for the entire engine/exhaust system including 1-step Arrhenius chemistry. The inclusion of chemistry introduces substantially more difficulty in obtaining stable solutions, especially for peak Mach numbers above ~1.5, possibly due to acoustic feedbacks.

This is an advantage of liquid-phase injective film cooling – the dilation resulting from vaporization of the coolant tends to suppress turbulent heat exchange

The results of running a similar model but with use of a thermo-chemical database and a simple, one-step chemical reaction  $CH_4 + 2O_2 \rightleftharpoons CO_2 + 2H_2O$  to study the ability of the PHOENICS solver to converge stressing combustion-chamber simulations with film coolants are shown in Figure 3..

A suggestion by Dr. Malin of CHAM was to include, via the PHOENICS InForm facility, the Sarkar compressibility correction for two-equation  $k-\epsilon$  turbulence modelling [11,12].

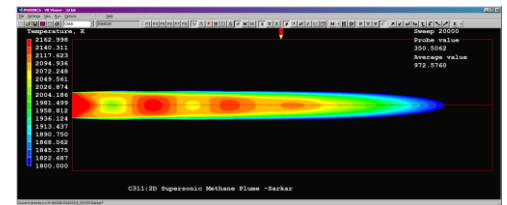
This correction has the effect of reducing turbulence-model-induced over-spreading of these flows.

We were not able to include this model in our engine chamber calculations due to difficulties encountered converging the chemistry solutions; however, we note here the InForm code, and, in passing, show some comparative results from the easy-to-converge PHOENICS Library case g11 (Figure 4).

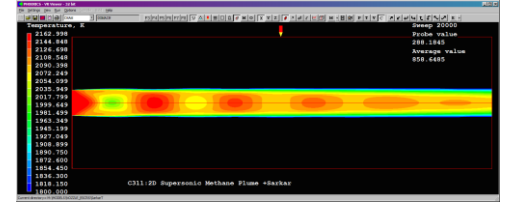
*This Newsletter comprises articles from PHOENICS Users describing work they have done, and are doing, with the Code.*

*The Spring Edition will contain articles from within CHAM and dates for the PHOENICS Diary in addition to further User contributions.*

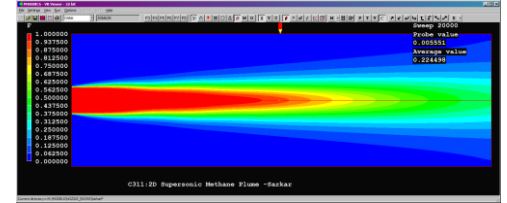
*Please send items for inclusion to [newsletter@cham.co.uk](mailto:newsletter@cham.co.uk).*



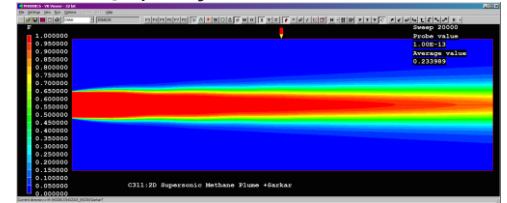
1: temperature without SC



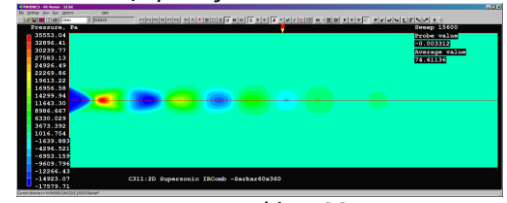
2: temperature with SC



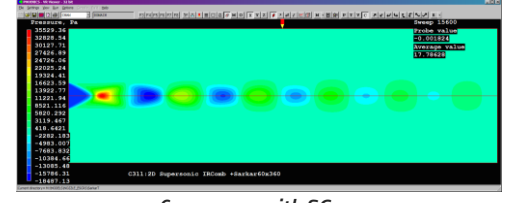
3: species fraction without SC



4: species fraction with SC



5: pressure without SC



6: pressure with SC

Figure 4. Converged steady axisymmetric solutions of post-nozzle flow from PHOENICS Library case g11 with added ESCRS model. The  $k-\epsilon$  turbulence model is used with and without the Sarkar correction (SC).

By providing whole-field storage for the variable MMWT, PHOENICS automatically calculates the mixture molecular weight from the thermo-chemical subroutine libraries when the Extended SCRS combustion model is used. The Sarkar correction code contains one empirical constant that controls the sink of turbulence energy due to dilatation dissipation, which the user may adjust ( $ALFE \approx 1.0$ ). It can be seen that simply including the Sarkar compressibility correction improves the number of shocks captured and

decreases the excessive spreading of the core species, as predicted. It is generally considered more valid to tune explicit model parameters (e.g., ALFE) than to arbitrarily adjust the standard turbulence-model coefficients of two-equation turbulence models.

Nonetheless, even though we cannot model the entire flowfield in a single simulation, the model results clearly show similar features to those experimentally observed in the LOX/kerosene rocket engine (Figure 1), suggesting our chamber calculations are on the right track.

### Summary

The persistence of the combustion-chamber film-coolant flow has a few immediate implications for the Earth's current fleet of space launch vehicles. First, in the lower stratosphere, the afterburning of the film coolant (and gas generator plume) ceases, which may extinguish soot formation resulting from afterburning of the thermally-converted film-coolant and gas-generator flows. The literature [4,5], public domain video data, and this work suggests that cracked large-molecule hydrocarbons (LMH) are thus the primary products dumped overboard with some engines.

Second, although the chemical effect of these LMH's on the upper atmosphere is currently unknown, it seems clear that they have orders-of-magnitude less anthropogenic solar-forcing than the equivalent mass of soot [7], which is often assumed to be the main byproduct of film coolants. Third, these results only hold for *film coolant* flows, which are not present in so-called  $N_2O$ /hybrid rocket motors, for which observed persistent soot is primarily the product of lower combustion efficiency as opposed to film-coolant flows.

Although it can be a challenge for the non-specialist to employ a CFD model such as PHOENICS to help understand observational data, it is clear that models such as PHOENICS are no longer entirely confined to the specialist CFD practitioner. Many practical problems can be understood with increased fidelity by the use of

software models, and codes are rapidly evolving to include increasingly robust features and standardized, community-validated configurations by which new, difficult problems may be modelled.

### References

1. AR5 Final Report, *Climate Change 2013: The Physical Science Basis*, [2013]  
[http://www.climatechange2013.org/images/report/WG1AR5\\_Chapter07\\_FINAL.pdf](http://www.climatechange2013.org/images/report/WG1AR5_Chapter07_FINAL.pdf)
2. UK Dept. for Transport, *UK Government Review of Commercial Spaceplane Certification and Operations*, Technical Report pp236 (and references thereon) [2014]
3. Spalding, D.B., et. al. *CHAM Technical Report: TR002*, Concentration, Heat & Momentum Limited, Bakery House, 40 High Street, Wimbledon, London SW19 5AU [2005]
4. Hartsfield, C. F., Ph.D. Dissertation, U.S. Naval Post Graduate School [2006]
5. Dellimore, K.H.J., Ph.D. Dissertation, University of Maryland [2010]
6. Ornellas, R., *EPG Space Design: the High-Reliability Tradeoff*, Cryogenic Biprop Rocket Engine Builders, Los Angeles, CA, USA; [epgspace@yahoo.com](mailto:epgspace@yahoo.com)  
<https://www.youtube.com/watch?v=wHLvIm72cMc>
7. Ross, M. and Sheaffer, P., *Earth's Future*, Volume 2, Issue 4, pages 177–196, [2014]
8. IPCC: <https://www.ipcc.ch/report/ar5/wg1/>
9. Sutton, G.P., *History of Liquid Propellant Rocket Engines*, AIAA, Reston VA [2006]
10. Simmons, F., *Rocket Exhaust Plume Phenomenology*, AIAA Press, 978-1884989087, [2000]
11. Sarkar, S., Erlebacher, G., Hussaini, M. Y., and Kreiss, H. O., *Journal of Fluid Mechanics*, Vol. 227, 473-493 [1991]
12. Wilcox, D. C., *AIAA Journal*, Vol. 30, No. 11, 2639-2646 [1992]
13. Malin, M.R., CHAM Technical Support, CHAM Ltd, London, UK, personal communication
14. Spalding, D.B., and Ludwig, J.C., *In-Form: CHAM TR-003*, Concentration, Heat & Momentum Limited, Bakery House, 40 High St, Wimbledon Village, London SW19 5AU [2006]

## Modelling Behaviour of Non-Metallic Inclusions in Steel Flows using PHOENICS

Peiyuan Ni, KTH-Royal Institute of Technology, SE-100 44 Stockholm, Sweden.

Non-metallic Inclusions in molten steel have received attention worldwide due to their serious influence on both the steel product quality and the steel production process. Inclusions can stop a continuous casting process by

clogging a tundish nozzle when they pass close to an inside nozzle wall and deposit onto the wall. Therefore, a good knowledge of both steel flow and inclusion behaviour is really important to understand nozzle clogging, as well as to take some possible measures to alleviate clogging.

### Turbulent Flow Phenomena and $Ce_2O_3$ Behaviour during a Steel Teeming Process

A three-dimensional model was developed to describe steel flow phenomena and inclusion behaviour during a teeming process.<sup>[1]</sup> The Kim-Chen modified  $k-\epsilon$  turbulent model was used to simulate the turbulence properties and the Height-of-Liquid model was used to capture the interface between gas and steel. A Lagrangian method, GENTRA in PHOENICS, was used to track an individual  $Ce_2O_3$  inclusion and to compare the behaviour of inclusions of different size in steel flow.

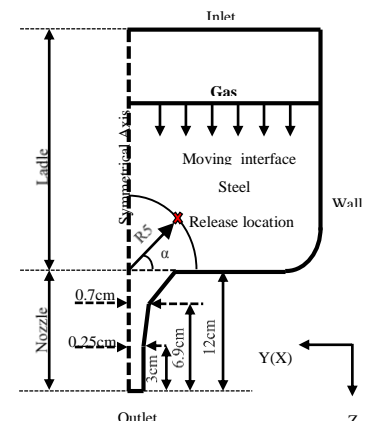


Fig.1 Schematic diagram of calculation domain and particle release location

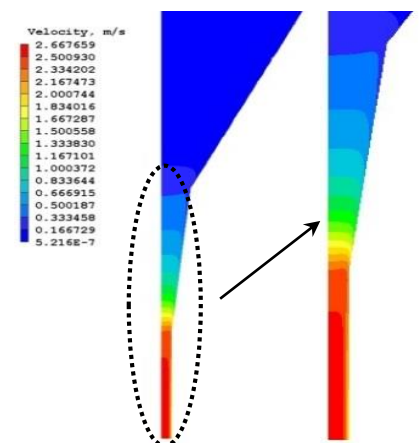


Fig.2 Steel velocity distribution in nozzle

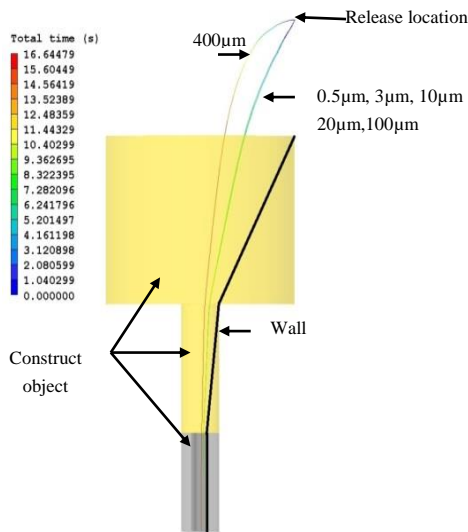


Fig.3 Trajectory of different-size inclusions in the nozzle

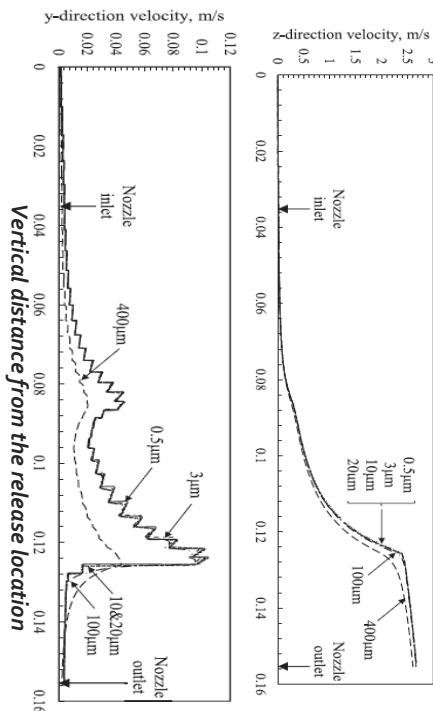


Fig.4 y-direction and z-direction velocity distributions of inclusions at different distance from the release location

Figure 2 shows information regarding steel flow in nozzles. Figures 3 and 4 show the behaviour of inclusions when they pass the nozzle. Different size inclusions behave differently; especially large inclusions due to their sizeable inertia.

#### Investigation of Nozzle Clogging during Continuous Casting of Steel

The Kim-Chen modified  $k-\epsilon$  turbulent model was used to simulate the turbulence properties in the tundish.

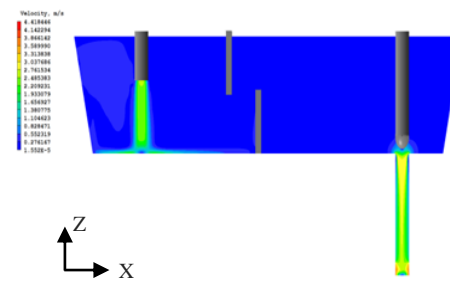


Fig.5 Steel flow field of a tundish during steel continuous castina

In order to know the deposition rate of non-metallic inclusions in the tundish nozzle, an Eulerian deposition model [2,3] was developed to predict the deposition rate. The analytical equations for deposition rates as a function of wall shear stress or friction velocity were written into PHOENICS using the In-Form function.

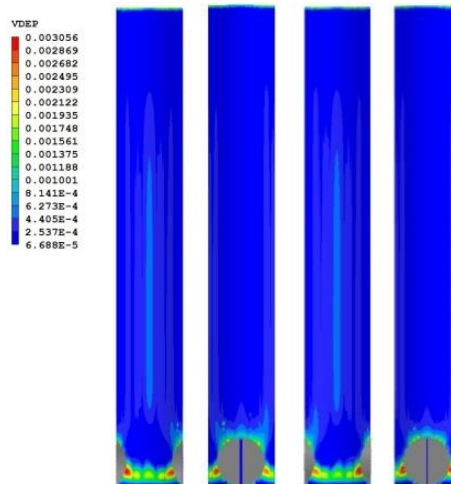


Fig.6 Deposition rates of inclusions of 5 µm at the inner surface of the tundish submerged entry nozzle

Fig.6 shows the non-uniform distribution of deposition rates of inclusions in the tundish nozzle.

#### References

- [1] P Ni, L T I Jonsson, M Ersson & P G Jonsson, ISIJ International, 53 (2013) pp 792-801
- [2] P Ni, L T I Jonsson, M Ersson & P G Jonsson, International Journal of Multiphase Flow, 62 (2014) pp 152-160.
- [3] P Ni, L T I Jonsson, M Ersson & P G Jonsson, Metallurgical & Materials Transactions B, 45 (2014) pp 2414-2424.



## Numerical CFD comparison of Lillgrund employing RANS

N. Simisioglou, S.-P. Bretonb, G. Crastos, K.S. Hansenc, S. Ivanellb  
WindSim AS, Fjordgaten 15, Tønsberg N-3125, Norway  
Uppsala University Campus Gotland, Visby SE 621 67, Sweden  
Technical University of Denmark, Nils Koppels Alle 403, Kgs. Lyngby DK 2800 Denmark

### Introduction

The current tendency towards ever growing offshore wind farms introduces the necessity of accurate wind-flow modelling of wind turbine wakes within the wind farm for layout optimization purposes. According to Dahlberg (2009), Lillgrund, an offshore wind farm located between Malmö and Copenhagen that consists of 48 2.3 MW Siemens wind turbines, has been found to have maximum peak losses occurring for the second turbine in the row and is for an inter-row spacing of  $4.4 \times D$  typically 70%, and for a row spacing of  $3.3 \times D$  typically 80%. Moreover, the turbine production efficiency rate for the entire wind farm has been found to be 67% if only below rated wind speeds are considered.

As the computational power of modern CPUs increases, previously impractical numerical CFD models are now being used by researchers and the industry to capture more accurately the wind flow within a wind farm. WindSim is a commercial wind farm development tool that solves the mass and momentum conservation equations by the Reynolds Average Navier Stokes (RANS) method using PHOENICS. The finite volume method is employed to discretize the RANS equations and the flow is assumed incompressible. The wind turbine rotors are modelled using the actuator disc method, meaning that the swept area of the wind turbine acts as a momentum sink extracting energy from the flow. In addition the thrust on the disc may be distributed with a uniform, parabolic or polynomial distribution and is calculated from the thrust coefficient curve of the turbine provided by the manufacturer.



The aim of this research is to validate the power production estimated using the actuator disc implemented in WindSim for each wind turbine against experimental data for the offshore wind farm Lillgrund.



Figure 1 Lillgrund Windfarm. Source Vattenfall

### Method

A grid sensitivity study was performed, and different parameters were investigated for their influence on the final power estimation. The parameters that were studied are two different thrust radial distributions, four different turbulence closure models and 21 different inflow directions. WindSim 6.0 was used where the RANS equations are solved using a coupled solver (Ferry, 2002). Different turbulent closures models were considered. Namely the  $k-\epsilon$  with YAP correction (Yap, 1987), the RNG  $k-\epsilon$  (Yakhot et al., 1992), the standard  $k-\epsilon$  and the modified  $k-\epsilon$  (Gravdahl, 1998).

### Conclusion

As one may see in Figure 2 and Figure 3 the results capture the power production of the wind turbines taking into account the wakes within the error bars of the experimental. Further the substantial decrease in power production of the second wind turbine due to the wakes of the first is captured. Concerning different turbulent closure models, it seems that the RNG  $k-\epsilon$  captures in some cases the power production reduction in the second wind turbine more accurately than the other turbulence models but underestimates the following wind turbines of the row.

On the other hand the standard  $k-\epsilon$ , modified  $k-\epsilon$  and  $k-\epsilon$  with YAP correction overestimate the power output of the second wind turbine in the row but capture the power loss for the subsequent wind turbines more accurately than the RNG  $k-\epsilon$ .

As a consequence future research will focus on the first three wind turbines in the row; accurate power estimates of the first three turbines seem to play a major role in accurately estimating the power production of all subsequent wind turbines in the row itself.

Furthermore research will be directed at how to include meandering and swirl effects in the wake model used in this analysis.

Finally, studies with higher grid resolutions and grid implementations will be conducted and comparison with analytical models and LES models will be performed.

Figure 2 Power predicted for four different turbulence models for a resolution of  $D/8$  versus experimental power data retrieved from Lillgrund for  $120 \pm 2.5$  degrees and  $9.0 \pm 0.5$  m/s for the polynomial distribution.

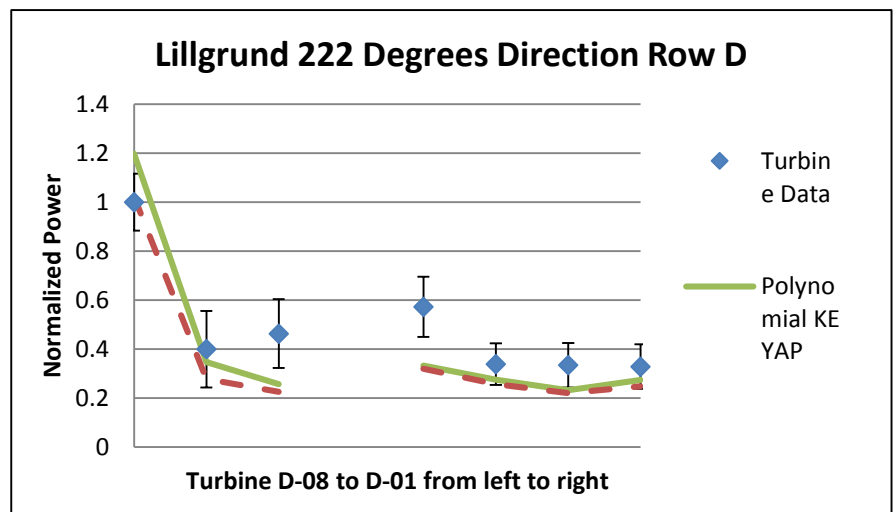
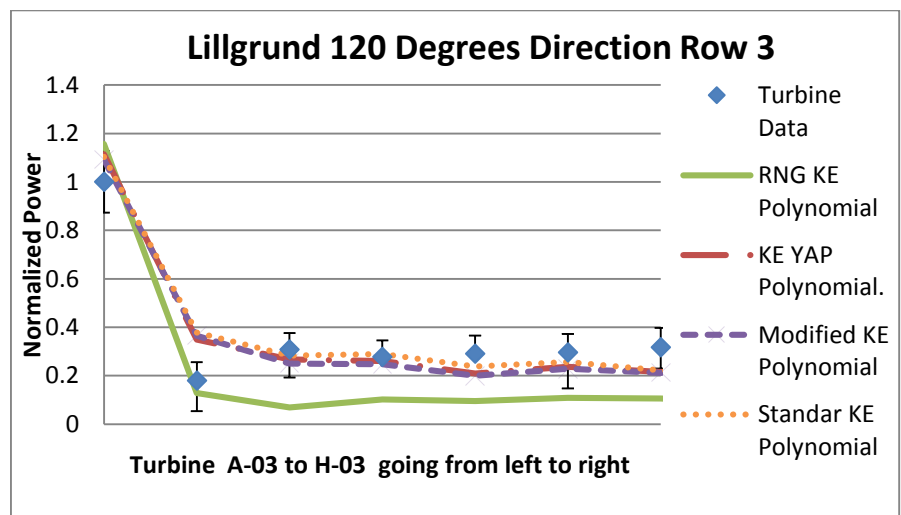


Figure 3: Power predicted by two different thrust distributions for a resolution of  $D/8$  versus experimental power data retrieved from Lillgrund for  $222 \pm 2.5$  degrees and  $9.0 \pm 0.5$  m/s when using the  $k-\epsilon$  with YAP correction turbulence closure model.

## References

1. Dahlberg, J.-A., 2009, Assessment of the Ilgrund Windfarm Performance Wake Effects Lillgrund, 6\_1 LG Pilot Report
2. Ferry, M., 2002. New Features of Migal solver. In: 9th International PHOENICS Users Conference. Moscow.
3. Gravdahl, A.R., 1998. Meso Scale Modeling with a Reynolds Averaged Navier Stokes Solver Assessment of wind resources along the Norwegian coast.
4. Yakhot, V., Orszag, S.A., Thangam, S., Gatski, T.B., Speziale, C.G., 1992. Development of turbulence models for shear flows by a double expansion technique. Phys. Fluids A Fluid Dyn. 4. 1520
5. Yap, C.J., 1987. Turbulent Heat and Momentum Transfer in Recirculating and Impinging Flows. PhD Thesis. U of Manchester.

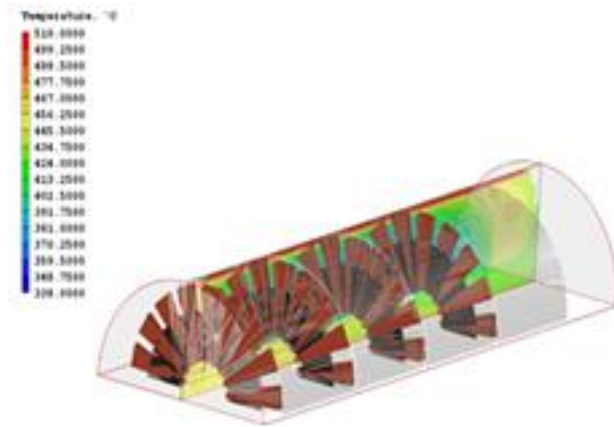
## PHOENICS use at Saudi Arabia Basic Industries (SABIC)

**Dr. Mansour N Al-Harbi, Staff Scientist, Saudi Basic Industries Corporation**

An engineering group, headed by Dr Mansour Al-Harbi, at SABIC's Technology Centre in Jubail, Saudi Arabia, has been using PHOENICS to model the processes involved during the batch annealing process.

Annealing is a heat treatment process widely used in the steelmaking industry to transform the product into a more ductile and useable form. This process is performed by heating the material for a prolonged period of time before cooling and is one of the critical unit operations involved in the production of cold rolled and annealed flat steel coils. It influences key plant performance parameters such as energy, productivity, and product quality.

In the batch annealing process, a typical set of 4-5 steel coils, separated by a convector plate, are piled on a furnace base. Sealed heated covers encloses the coils where an inert gas is circulated.



Due to the mass weight of the coil, hot and cold spots would be generated. The batch annealing cycle is designed to homogenise the coil temperature, which control the product quality and mechanical properties.

During 2013, CHAM's technical support team provided assistance to SABIC personnel in the development of their 'batch annealing furnace' model.

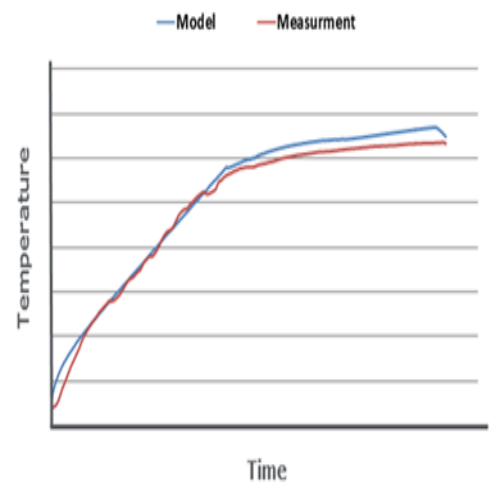
The PHOENICS-based CFD model simulated a batch-type annealing process that consists of stacking multiple coils within an inner cover filled with hydrogen gas. A furnace surrounds the inner covers with the use of burners, and heat is forced through the coils by a fan circulating the gas inside the inner cover.



To obtain a better understanding of the current annealing process, which influences cycle time and coil temperature uniformity, PHOENICS was employed to simulate the heating cycle of the batch annealing furnace.

The simulation results presented detail transient-flow velocity and temperature distributions within the inner cover and the coils to achieve a thorough understanding of the gas flow pattern and heating process

The CFD model produces excellent agreement with measurements taken at the plant, as shown.



As reported in the Autumn issue of PHOENICS News, SABIC has also worked with CHAM to develop a 3D transient "furnace re-heating" model.

This starts with a steady state solution to develop the gases flow pattern coming out from the burners and to establish the different temperature zones within the furnace chamber. Then, a transient solution is initiated to simulate the entrance of new billets into the furnace and their movement inside.

Each billet spends around one minute at each location before it finally leaves the furnace. The CFD model is intended to provide the temperature evolution of each billet throughout its 1-hour journey inside the furnace.

See:  
<http://www.cham.co.uk/DOCS/PHOENICS-News-Autumn-Winter-2013.pdf>

Once fully developed, SABIC intends to use both CFD models further to optimise the physical production process.

## PHOENICS Post-Processing of additional variables via Python scripts

Venugopalan Raghavan,  
Zeb Technology, Singapore

One of ZEB-Technology's recent projects required computations of additional variables after the runs had finished. One approach was to restart the simulations and define the variables with IN-FORM commands and run the simulation for a couple of steps.

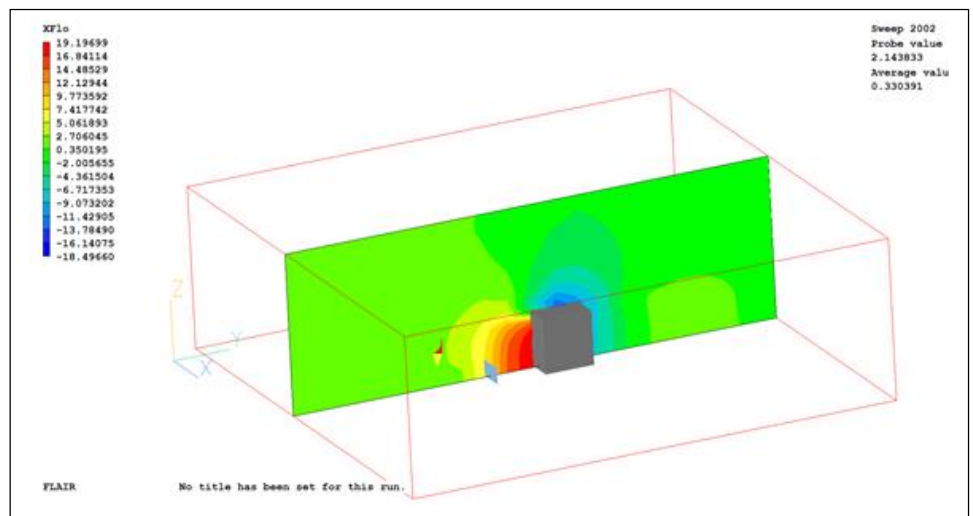
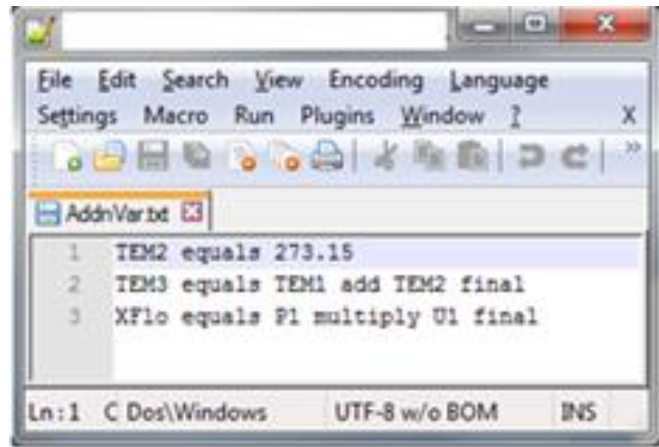
While this would be relatively straightforward to do, ZEB understood from CHAM that special care would need to be taken with relaxation parameters for the restart in order to avoid problems with convergence.

As the computations were already available, ZEB-Technology decided to work on a Python script that would read in definitions of additional variables, compute the values for these additional variables and write them out to a different phi files without having to worry about overwriting the original case or waiting to restart and rerun the simulations.

This script does not and will not solve for the fundamental variables. It only works on the final PHI file and is written for the sole purpose of helping with further post-processing.

Currently the Python script handles only basic arithmetic operations – addition, subtraction, multiplication and division; only one operation is allowed per line and needs to be written in a text file. It is hoped to increase the complexity that the script can handle over the next few iterations of the script. At the moment it has been tailored for the PHI file and consequently cannot handle PHIDA files.

Below is an example of an extra variable "XFlo" that was computed using the Python script



The developed script provides an additional way to generate extra variables for plotting, especially where the extra variables are derived from simple arithmetic operations of the main variables which are output by PHOENICS, serving as a value add that can save on time.

## SketchUp↔PHOENICS conversion tool

Venugopalan Raghavan  
Zeb Technology, Singapore

In many cases, it is preferred to draw building geometry in a CAD based toolkit such as AutoCAD or SketchUp. These packages are popular with a large user base more at ease with these commercial software packages.

For highly complicated geometry, STLs can be imported separately. However, for standard PHOENICS objects like inlets and outlets which

are sometimes required to be placed at specific locations and/or distances, geometric operations are better being completed in a CAD environment rather than in PHOENICS.

A Ruby script was developed to write each SketchUp group along with its properties (inlet, blockage etc.). A Python script then takes this output to write a q1 file that can be read by PHOENICS.

Similarly, a script first to convert PHOENICS objects into a collection of points and surfaces is written and then read by a Ruby script file to create the geometry in SketchUp.

This script allows users with an architectural background quickly to create geometries in their preferred environment and use these scripts quickly to get their geometry for use in PHOENICS. Likewise, exporting PHOENICS cases into SketchUp helps facilitate further analysis for building performance such as energy analysis with IES or similar.